Novel Direct Synthesis of Mesoporous Tin Dioxide Network Intact up to 500 °C

Tariq Aqeel*[1], Heather F. Greer[2], Wuzong Zhou[2], Duncan W. Bruce[3], Ali Bumajdad[4]

[1] Science Department, College of Basic Studies, the Public Authority of Applied Education and Training (PAAET) P.O Box 23167, zip code Safat 13092, Kuwait. tm.aqeel@paaet.edu.kw

[2] School of Chemistry, University of St Andrews, St Andrews, KY16 9ST UK.

[3] Department of Chemistry, University of York, Heslington, YORK YO10 5DD, UK.

[4] Chemistry Department, Faculty of Science, Kuwait University, P.O.Box 5969 safat 13060, Kuwait.

Abstract

We present a direct soft templating method to synthesise mesoporous tin dioxide network that maintains a porous structure after calcination at 400 °C and 500 °C and has a relatively high BET surface area of 220 and 100 $m^2 g^{-1}$, respectively. TEM, BET and XRD results confirm that both crystal and pore sizes increase as a result of increasing the temperatures during the calcination step. This method is highly reproducible.

Key words:

Mesoporous tin dioxide, TEM, BET, XRD, XPS, pore and crystal sizes, calcinations.

Introduction

Tin dioxide is an n-type semiconductor having a band gap energy around 3.6 eV [1] and can be used in various applications such as gas sensing, [2-5] as an electrode in galvanic or electrolyte cells, [6,7] transparent electrode in solar cell and photocatalysis. [8-9] As a solid it forms a powder having a surface area in the range of 10-30 m^2g^{-1} and this low surface area limits its applicability as a sensor or electrode. Introducing porosity into its structure will increase the surface area and pore volumes significantly. Thus, many publications report the production of mesoporous tin dioxide, but they often been supported by substrates [10-13], sometimes lack reproducibility [14-15] or the product was supported by soft [16] or hard templates which were not removed completely. [14-15] We have recently tried to reproduce some of the published methods to synthesise mesoporous tin dioxide powders (free of the supporting substrate or the templating materials) using their procedures, but in our hands the methods were not reproducible, [14-15] for example, using hard templating materials such as mesoporous silica [14-15]. Here we found that under all conditions that we employed, the product always contained between 5 and 15% residual mesoporous silica which may in fact be a significant source of the high surface area (100 $m^2 g^{-1}$) claimed for the materials. [14-15] Other

methods, for example using a soft templating support, [17], led to pore structure collapse after calcination at 400 °C, giving a non-porous powder. However, based on our experience, we can manipulate this latter method to produce mesoporous tin dioxide powders free of the templating materials at elevated temperatures.

Based on a previous method, [17] we developed a methodology that gave mesoporous tin dioxide after calcination at 400 °C and 500 °C. Moreover our product could withstand multiple heat treatments without losing this porosity, providing a good basis for the subsequent, post-synthetic introduction of nano-clusters into the pores or doping of the walls with other elements to modify chemical and physical properties. The method employed is highly reproducible.

Results and Discussion

Synthesis

Previous reports mixed the reagents without stirring for two days before removing the surfactant (tetradecylamine) by heating the product in ethanol under reflux for two hours (to remove the template) before calcining. This resulted in formally microporous materials, pore diameters of 14 Å and 18 Å arising from calcination temperatures of 300 and 350 °C, respectively. The present methodology used slow stirring (around 100 r.p.m.) and increased the reaction time to three days to ensure good mixing and to produce thicker walls and then the surfactant (hexadecylamine) was removed using Soxhlet extraction with ethanol for 16-20 hours. This led to materials with an average pore diameter of 20 Å and 22 Å following calcination at 300 °C or 400 °C, respectively.

X-ray Diffraction

Figure 1 represents the small-angle diffraction pattern for mesoporous SnO_2 calcined at different temperatures. The small-angle reflection indicates that all have some structured porosity and, while this appears best defined at 400 °C, it evidently extends to the sample treated at 500 °C. Moreover, the fact that the *d*-spacing increases with calcination temperature (49 Å, 77 Å and 98 Å at 300 °C, 400 °C and 500 °C, respectively) suggests that the structure is changing by having thicker walls and/or larger pore sizes.

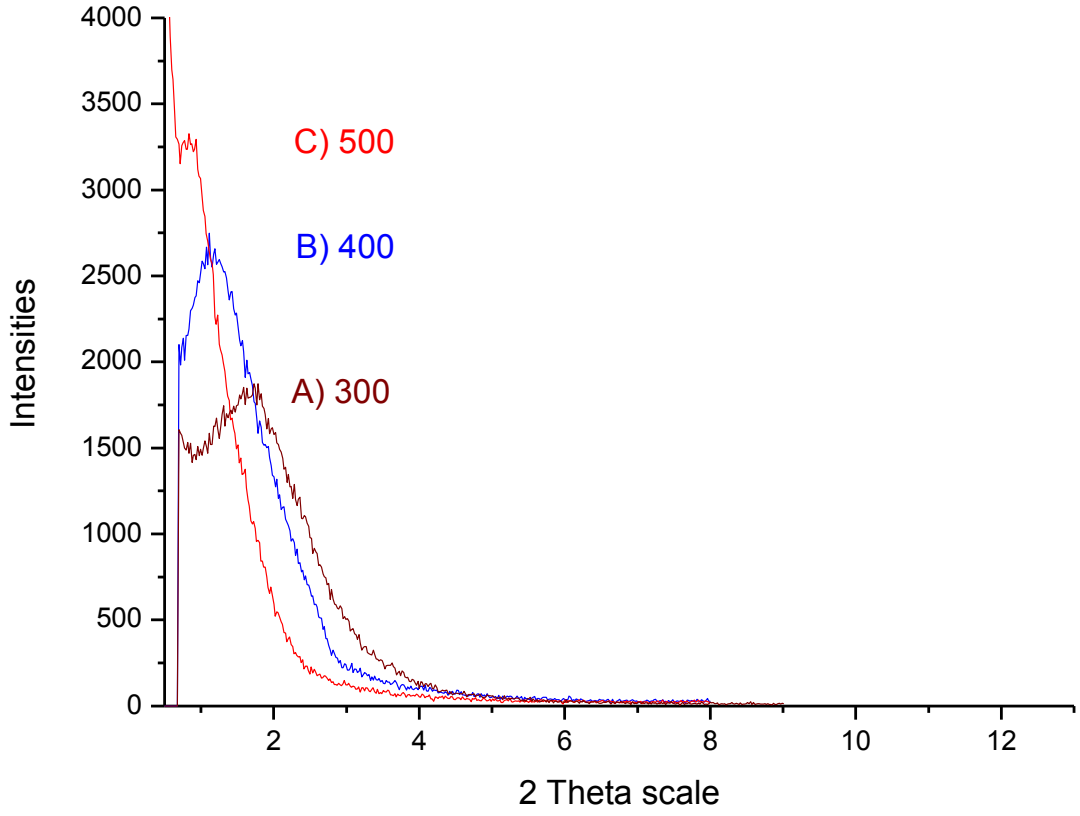

Fig.1 Small-angle XRD diffraction patterns for mesoporous SnO_2 calcined at:
A) 300 °C, B) 400 °C and C) 500 °C

The wide-angle diffraction patterns (Fig. 2) confirm that all samples are crystalline and the structure is assigned as Cassiterite by comparison with library data.[1] Moreover the wide-angle data show that the crystallinity is improving as the temperature increases by having sharper and narrower peaks which are more pronounced at 400 °C and 500 °C than at 300 °C. Furthermore the crystal size increased as a result of the increase in the calcination temperature as evaluated using the Scherrer equation for the <110> reflection, so that the average crystal sizes are calculated to be: 34 Å at 300 °C, 52 Å at 400 °C and 72 Å at 500 °C. Many other papers also reported the increase in particle size as a direct result of increasing the temperature. [18-20]

[1] *EVA* software associated with *D8* advanced diffractometer DIFFRAC^{plus} XRD instrument.

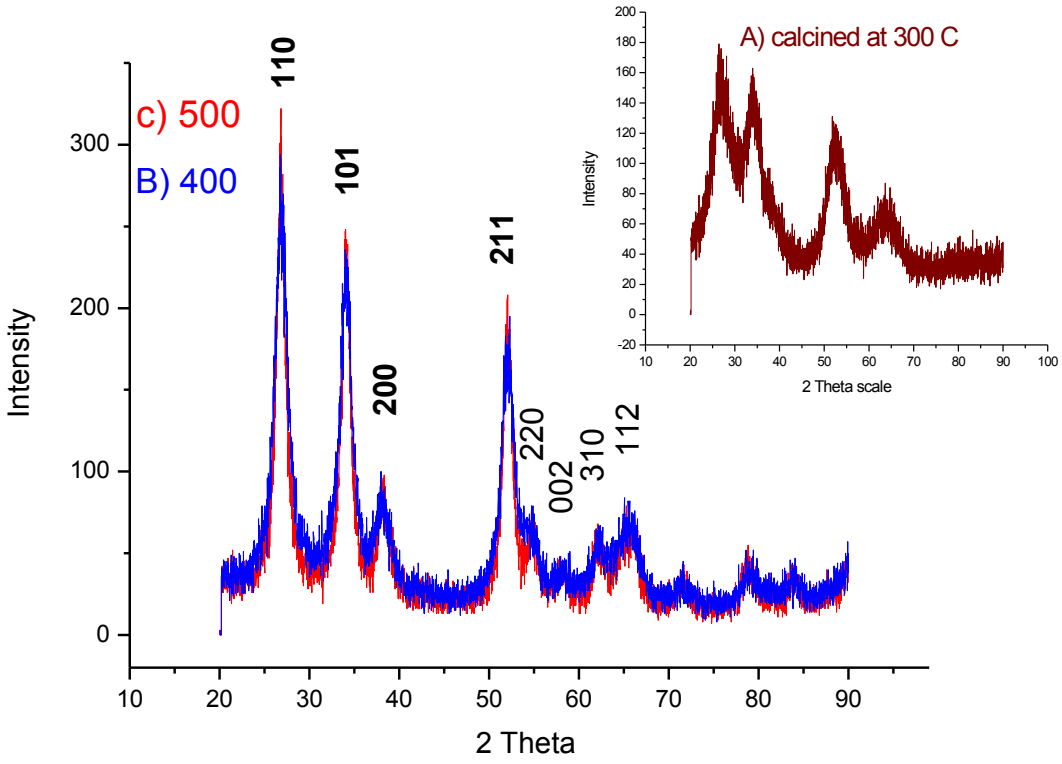

Figure 2 The wide-angle XRD patterns for samples A, B and C calcined at the indicated temperatures.

BET results

Brunauer-Emmett-Teller (BET) N_2 sorption measurements were performed to study the removal methods of the templating materials and the effect on the product. The removal of the templating materials was performed either by heat treatment alone or by Soxhlet extraction using ethanol followed by heat treatment which reveals the following results.

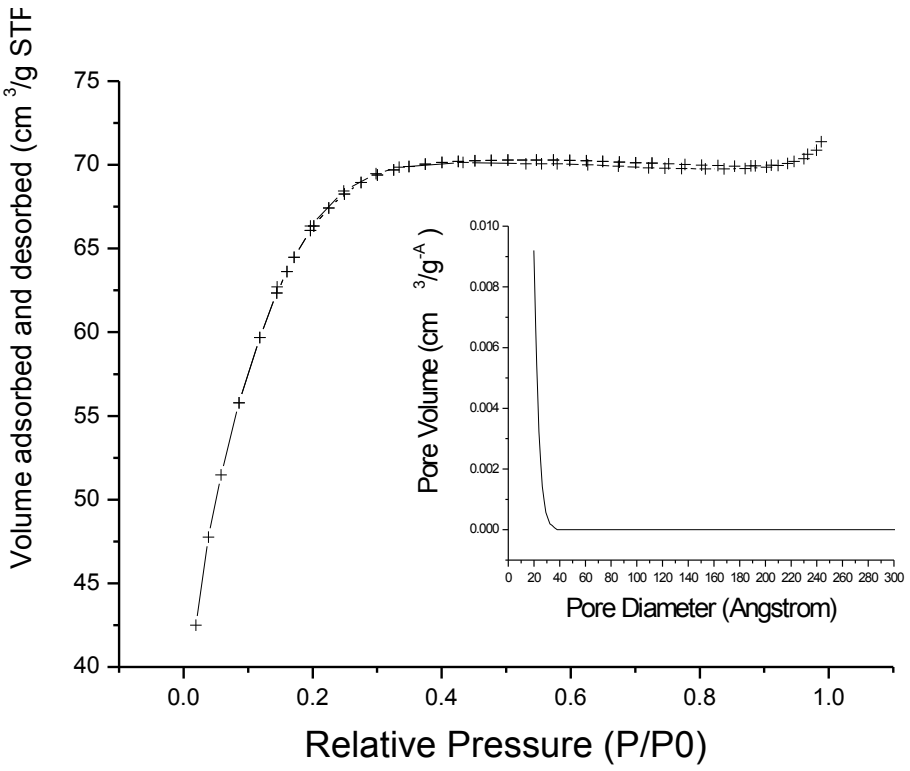

(a)

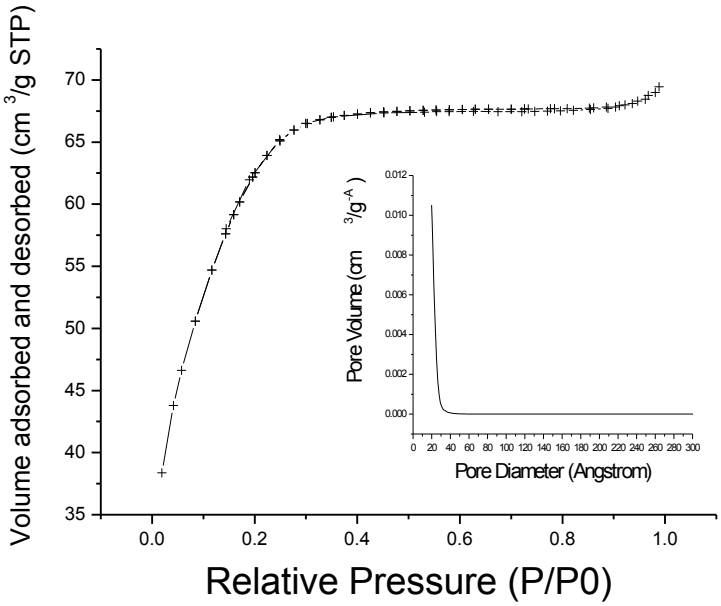

(b)

Figure 3 The isotherm for porous tin dioxide (a) calcined at 300 °C and (b) Soxhlet extracted for 16-20 h then calcined at 300 °C.

For heat treatment at 300 °C, one batch was divided into two samples and the removal of the templating material of the as-synthesised product was performed differently. The first sample was washed in water, rinsed with ethanol then calcined at 300 °C for 2 hours (Fig. 3a), whereas the other was treated in a Soxhlet ethanol extraction for 16-20 hours then calcined at 300 °C for 2 hours (Fig. 3b). Both samples showed similar isotherms (Type I which indicates microporosity of pore size < 2 nm) and BET results show pore volumes of 0.1 $cm^3\ g^{-1}$, BET surface areas of 230 m^2g^{-1} and uniform pores in the 20 Å range, which fall in the borderline between micro- and meso-porosity according to IUPAC classification. [21]

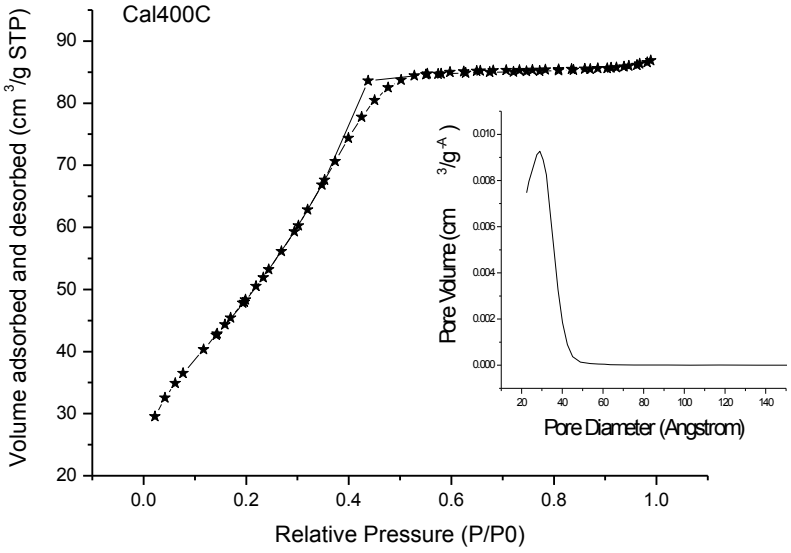

(a)

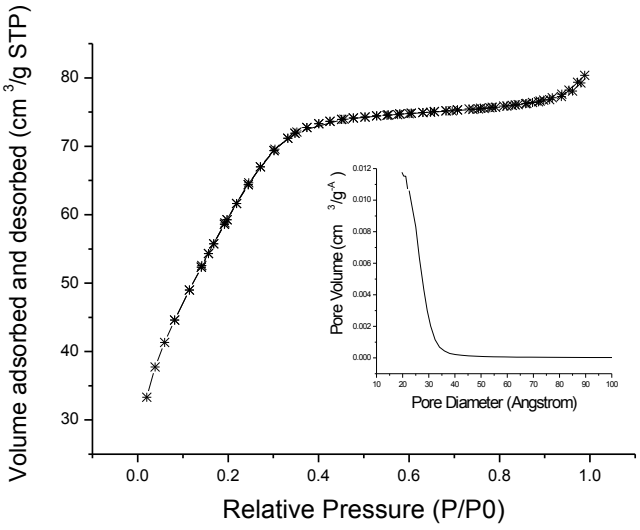

(b)

Figure 4 The isotherm for tin dioxide (a) calcined at 400 °C;
(b) Soxhlet treated then calcined at 400 °C.

Two further batches were treated similarly, only this time the calcination temperature was 400 °C. Thus while the sample that was subjected to Soxhlet extraction followed by calcination again showed a Type I isotherm, the sample that was simply calcined showed some evidence of hysteresis suggesting a possible Type IV isotherm (hysteresis loop type H2) and mesoporosity. Indeed, the pore size for the calcined sample averaged a diameter of 29 Å with a surface area of 179 $m^2 g^{-1}$. When extracted and then calcined, the pore diameter reduced to 22 Å, there was no hysteresis loop and the surface area was 221 $m^2 g^{-1}$.

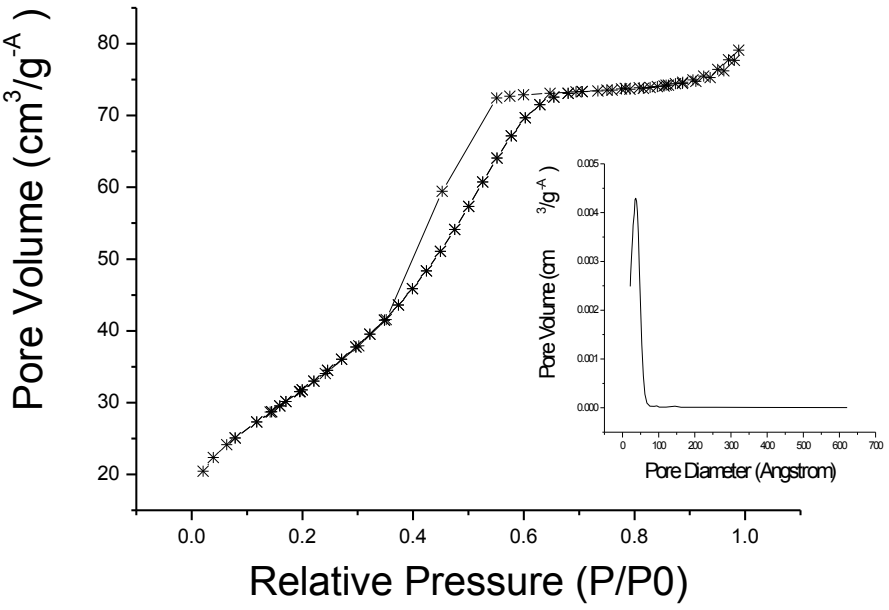

Figure 5 The isotherm for mesoporous tin dioxide Soxhlet treated then calcined at 500 °C

For heat treatment at 500 °C, we know that the crystal size of tin dioxide will increase directly with the heat reducing the size of the pores. [18]. We therefore decided to use Soxhlet extraction with ethanol for 16-20 hours for template removal before calcining hoping to maintain the porous structure intact. Thus, we calcined at 300 °C for 30 minutes, at 400 °C for a further 15 minutes (ramp rate = 2 °C min^{-1}) and then at 500 °C for 10 minutes (ramp rate = 3 °C min^{-1}). Best results gave a BET surface area of 116 $m^2 g^{-1}$, a pore volume of 0.12 $cm^3 g^{-1}$ and an average pore diameter of 56 Å. The hysteresis loop (falling between the H1 and H2 IUPAC classification) of the desorption cycle was more pronounced indicating larger pore size distribution ranging from 26 - 66 Å as presented in Fig. 5. Class H1 hysteresis is defined as arising from cylindrical pores whereas H2 type hysteresis represents an interconnecting pore system or irregular shape pores [21]; our TEM results are consistent with both. Other samples similarly prepared had comparable results with average BET surface area around 100 $m^2 g^{-1}$.

The heat treatment of the samples produced larger pore sizes, ranging from 20 to 60 Å as a result of the calcinations temperature increment. These results observed by BET data agree with the increase in the *d*-spacing value calculated from the XRD spectrum (Fig. 1).

TEM results

The low-magnification TEM image (Fig. 6a) of the SnO_2 sample calcined at 400 °C shows a network of spherical-like particles (*ca* 300–500 nm). The high porosity of these spherical particles can easily be identified in higher-magnification images (Fig. 6b). HRTEM confirmed that the spherical particles were built up of nanocrystallites with a dimension of 4–5 nm (Fig. 6c). The marked lattice fringes in **Fig. 6c** with *d*-spacings close to 3.34 Å match to the (110) plane of SnO_2 (cassiterite). The pores are actually the space in between the nanocrystallites and are, therefore, irregularly shaped and disordered due to the non-uniform arrangement of nanocrystallites. High intensities of Sn and O in the EDX spectrum (inset of Fig. 6c) further supports identification of the SnO_2 phase and confirm its purity. The Cu in this spectrum is from the copper grid on which the specimen was deposited.

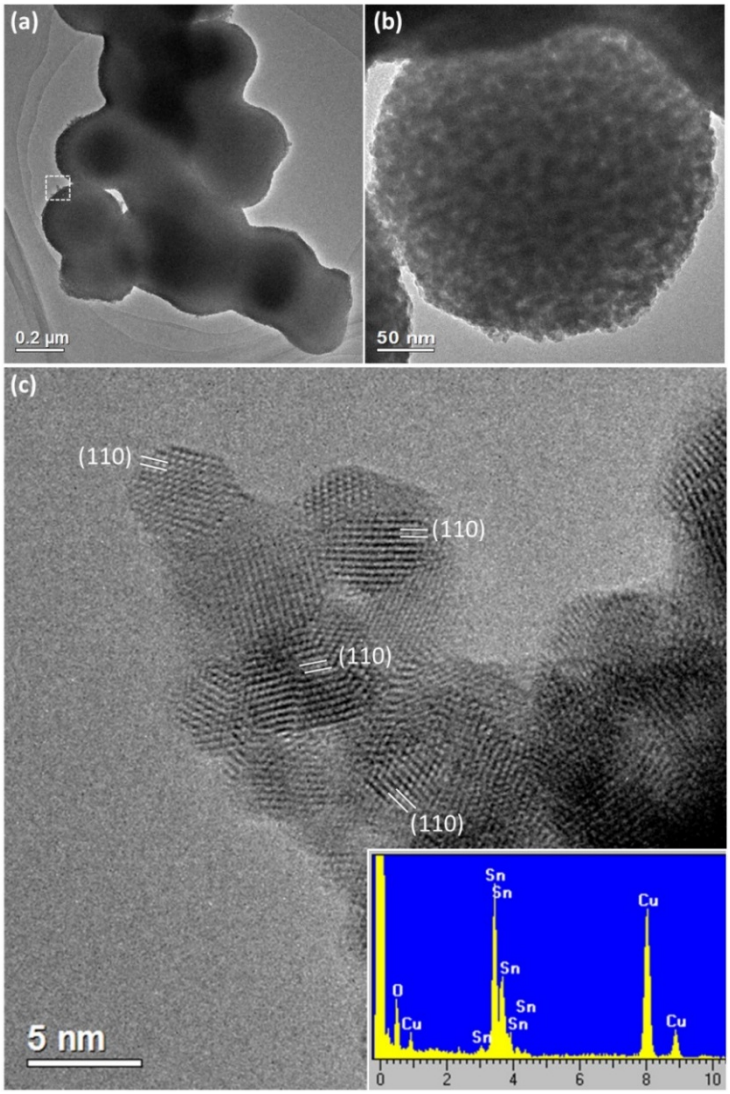

Figure 6 TEM images of mesoporous SnO_2 calcined at 400 °C: (a) Low-magnification TEM image showing spherical particles with a network-like arrangement; (b) TEM image showing the spherical particles have a porous structure consisting of nanocrystallites; (c) HRTEM image recorded from the area marked in (a). The *d*-spacings measured from many nanoparticles corresponds to the (110) plane of SnO_2. A typical EDX spectrum of this specimen is shown in the inset.

Similarly, low-magnification TEM images (Fig. 7a) of the SnO_2 specimen calcined at 500 °C also show a network structure but with a smaller size, *e.g.* 200–250 nm, of spherical building units. Many nanocrystallites could also be observed at slightly higher magnifications (Fig. 7b). The visibility of many pale contrasted voids in low-magnification TEM images of the specimen calcined at 500 °C (Fig. 7a), but not 400 °C (Fig. 6a), is consistent with the average pore size data. The HRTEM image in Fig. 7c confirmed that the nanocrystallite size is 6–9 nm, which matches with that obtained from Scherrer calculations. It is noted that the nanocrystallites in the specimen calcined at 500 °C are larger and have defined facets; the majority are (110), whereas the smaller crystallites in the 400 °C sample are spherical and without obvious facets. All marked lattice fringes in Fig. 7c correspond to

the (110) plane of SnO_2 with a *d*-spacing close to 3.34 Å. A typical EDX spectrum of the specimen calcined at 500 °C, displaying only high intensities of Sn and O, is shown in the inset of Fig 7c. Despite the disordered arrangement of nanocrystallites in both the 400 °C and 500 °C specimens, the connection between the nanocrystallites are evidently relatively strong otherwise a network structure would not be possible.

Based on the TEM results the porous structure is similar to single crystalline metal oxides produced using mesoporous silicas as hard templates [22], although the pores in SnO_2 are irregular and the wall is polycrystalline rather than single crystalline. The network structure also indicates that the formation of these materials is not resulted from aggregation of pre-formed nanocrystallites. The precursor molecules/ions aggregate into some amorphous spherical particles first, followed by multiple nucleation and development of nanocrystallites in the particles simultaneously. Consequently, the connection of the nanocrystallites is chemical rather than physical. A comparable mesostructured is the so-called walnut-like perovskite [23].

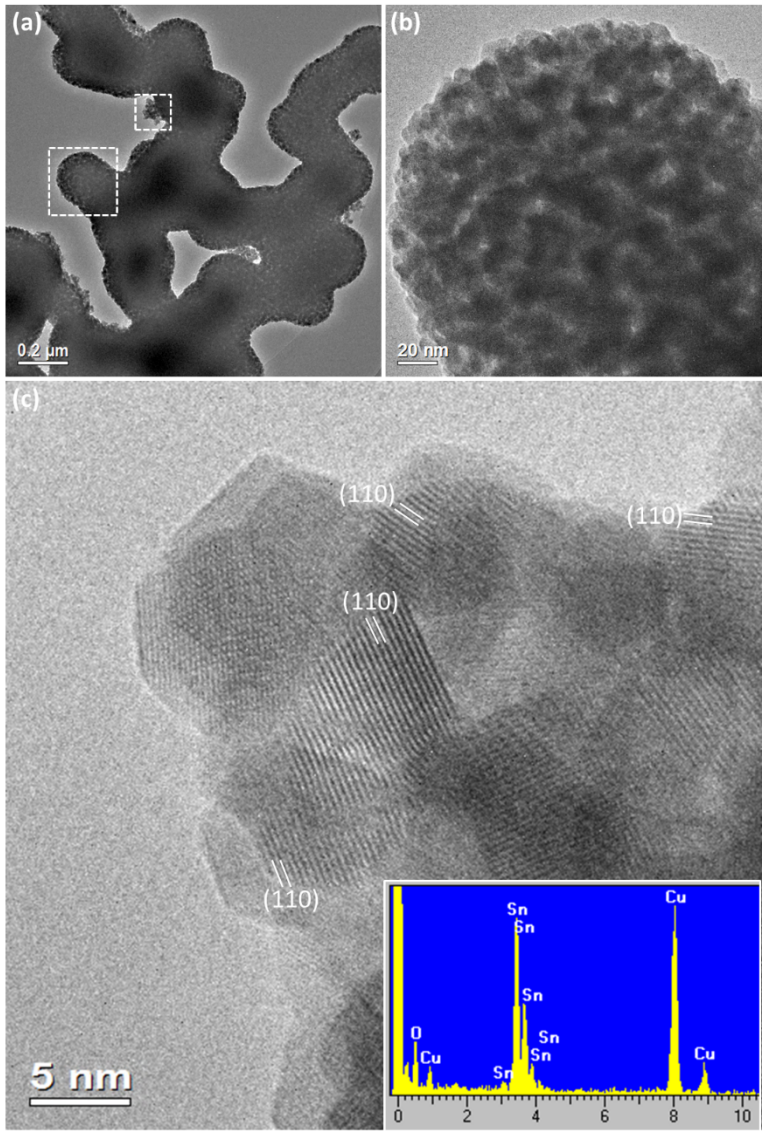

Fig. 7 TEM images of mesoporous SnO_2 calcined at 500 °C: (a) Low-magnification TEM image showing a network type structure; (b) higher-magnification TEM image recorded from the area marked by a large box in (a) – a highly porous structure consisting of nanocrystallites can be identified; (c) HRTEM image recorded from the smaller marked region in (a) – the marked lattice fringes have *d*-spacings that correspond to the (110) plane of SnO_2. The inset shows a typical EDX spectrum recorded from this specimen.

XPS results

The X-ray Photoelectron Spectrometry (XPS) data, presented in Figure 8 and Table 1, reveal that the total carbon content is 1.56% for the sample calcined at 500 °C and 1.88% for the sample calcined at 400 °C. Subtracting 1.21 and 1.25 atom% from the total carbon as being adventitious, for the samples calcined at 500 and 400 °C, respectively, the resultant levels are 0.35 and 0.63 atom% C for the samples calcined at 500 °C and 400 °C, respectively. This arises from residual carbon from the starting template and is lower for the higher calcination temperature. [24] Detected surface nitrogen atoms are from the starting templating material and the content was 0.2% for the sample calcined at 400 °C and 0.1% for that calcined at 500 °C. Both the carbon and the nitrogen results confirm the removal of the templating materials and show that the mesoporous tin dioxide structure exists intact without the support of the carbon templates. Moreover 50.0% of Sn atoms exist in the framework as tin dioxide as represented by Sn3d3/2 and Sn3d5/2 peaks. The peak symmetry, the binding energies values, and the spin-orbit splitting (8.4 eV) fit well with that found in the literature and indicates that the tin is of pure tetravalent oxidation state (Sn^{4+}). [25] Oxygen atoms are about 48.0 atom% and exist in the framework mainly as tin dioxide. [24] The presence of two type of oxygen (small amount of OH^- around 531.6 eV and a majority of O^{2-} around 530.6 eV) indicate that the surface layers consist of some hydroxide form and/or physisorbed water vapour. This hydroxide is less for the 500 ^{o}C-calcined sample (see Fig. 8).

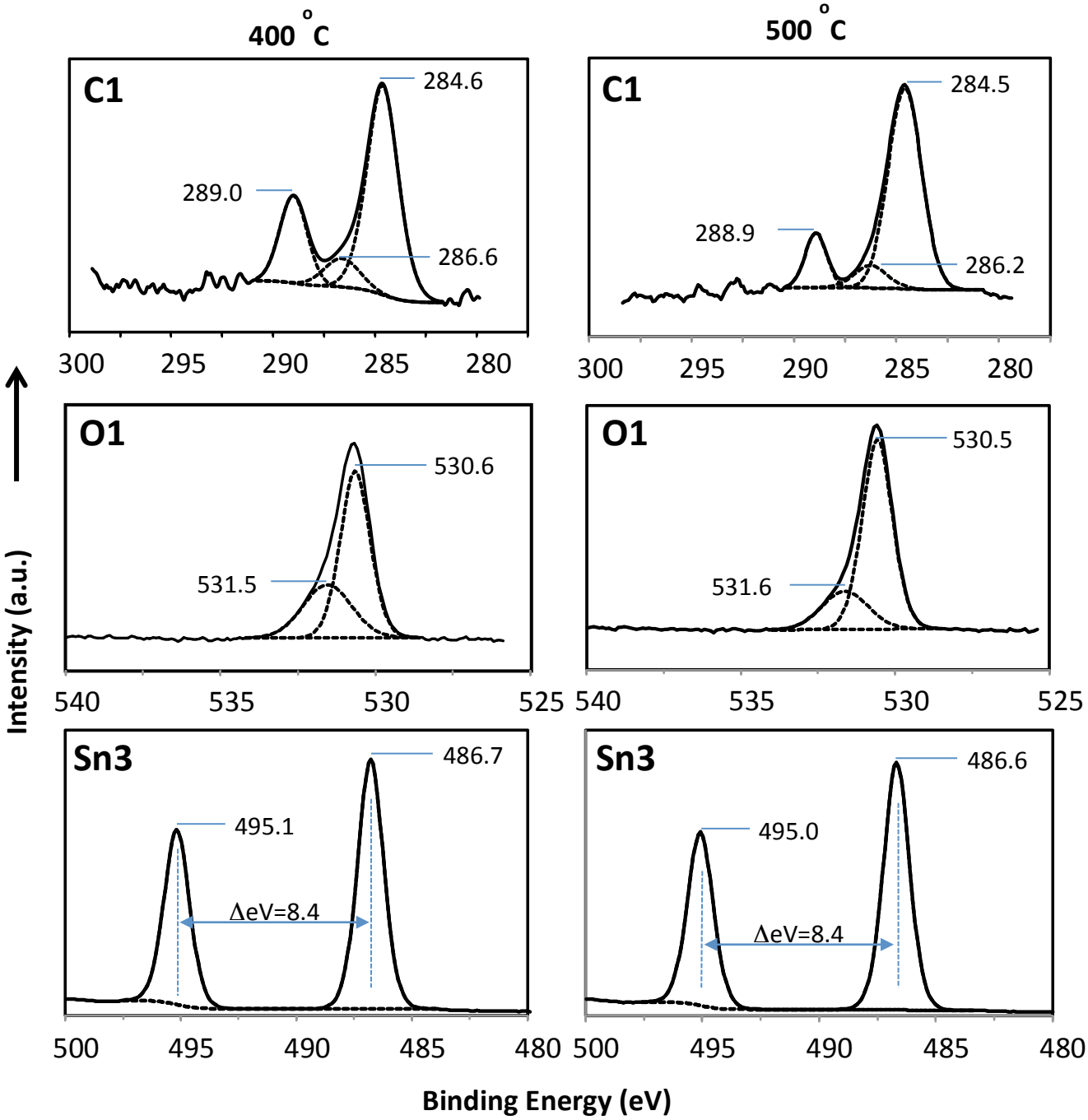

Figure 8 Deconvoluted C1s, O1s and Sn3d XPS spectrum. Sample calcined at 400 °C (left); sample calcined at 500 °C (right).

Table 1. XPS Elemental and Quantification for samples calcined at 400 °C and at 500 °C

Peak (400 °C sample)	BE/eV	Intensity/Counts	FWHM/eV	Atom %	*Q*
N1s	400.36	74.22	2.1	0.26	1
C1s	*284.63	306.38	1.81	1.25	1
C1s A	289.01	127.67	1.58	0.44	1
C1s B	286.63	42.18	2.04	0.19	1
Sn3d5	486.78	139750.08	1.29	24.95	1
Sn3d3	495.18	97875.59	1.28	25.08	1
O1s	530.66	31326.88	1.12	31.47	1
O1sA	531.56	10002.46	1.84	16.18	1
Peak (500 °C sample)					
N1s	400.53	66.55	1.73	0.12	1
C1s	*284.51	396.97	1.91	1.21	1
C1sA	288.93	107.68	1.23	0.21	1
C1sB	286.26	44.53	1.88	0.14	1
Sn3d5	486.68	190376.42	1.29	24.62	1
Sn3d3	495.09	133297.92	1.28	24.71	1
O1s	530.57	50115.93	1.14	37.17	1
O1sA	531.63	10103.21	1.76	11.33	1

*Binding Energy at 284.6 eV represents adventitious carbon

Conductivity results

Conductivity measurements were carried out using two banana cables at room temperature. It was not possible to construct a device to measure conductivity at elevated temperature as every time the temperature was increased, the resistivity of the metallic wires connected between the sample and the probes increased and, as a result, the total conductivity of the system decreased. Readings taken at room temperature gave an average result of 54×10^{-3} S m^{-1} for the sample calcined at 400 °C and 164×10^{-3} S m^{-1} for the sample calcined at 500 °C. Both samples confirm that the mesoporous tin dioxide classifies as a semiconductor and conductivity is predicted to increase with an increase in temperature.

Conclusion

Mesoporous tin dioxide powder has been prepared *via* a direct soft templating method which is highly reproducible. The porous structure is able to withstand calcination at 400 °C and 500 °C and shows high BET surface areas of 220 and 100 m^2 g^{-1}, respectively. The crystal and pore sizes increase as a result of increasing the temperature during the calcination step, explaining why an increased

dwell time is essential to control the sample morphology and prevent total collapse of the structure into a dense oxide of low surface area.

EXPERIMENTAL

Characterisation

X-ray diffraction performed using Bruker AXS D8 advanced diffractometer, using a copper target (λ = 1.5418 Å) and DIFFRAC^{plus} software. The surface areas of the calcined samples were determined by BET adsorption-desorption measurement on a Micrometrics Tristar analyser, using nitrogen as the adsorbing gas. Transmission electron microscopic (TEM) images were attained using a JEOL JEM-2011 electron microscope operated at 200 kV. The TEM images were recorded using a Gatan 794 CCD camera. This electron microscope is equipped with an Oxford Link ISIS SemiSTEM EDX system, which was used for confirming the chemical compositions at University of St Andrews. Conductivity measurements were performed using Agilent B2901A Source/Measure Unit (SMU) and two banana probes at 4 mm distance a part 42V, 102 mA at room temperature. The X-ray photoelectron spectroscopy (XPS) spectra were recorded on a model Thermo ESCALAB 250Xi spectrometer using a monochromator with Al Kα radiation (1486.6 eV). The spectra acquisition and processing were carried out by means of Avantage data system. Sample was carefully introduced into the preparation chamber with the sample holder. It is then degassed until a good vacuum is achieved, then it was transferred into the analysis chamber. The analyses were carried out with the parameters: Analysis chamber pressure 10 -9 Torr, step size 0.1 eV, dwell time 100 ms, and pass energy of 20 eV. All binding energy values were determined with respect to °C1s line (284.6 eV) origination from adventitious carbon. Flood gun with standard charge compensation mode was used to neutralize the charge build up on the surface of insulating samples.

Preparation

Mesoporous SnO_2 was prepared by slow stirring hexadecylamine (0.26 g) mixed in ^{i}PrOH (24.4 cm^3) until dissolving completely then $Sn(O^{i}Pr)_4$ (1.9 g) added at room temperature giving molar ratio of 0.2: 60:1 respectively. The reaction left under water-saturated air (about 80% humidity) for three days, the product was filtered and washed with water and then ethanol. Then transferred to Soxhlet extraction using ethanol, as a solvent, left over night (about 16 h) to remove the surfactant then filtered. The product was calcined at temperature of 300 °C, 400 °C and 500 °C in air (heating rate 2 °C min^{-1}) for periods mentioned in the text.

All Chemicals where used as purchased from Alfa Aesarand used with good chemical practices.

Acknowledgment

This project is supported by PAAET project no. BE-13-08 in collaboration with Kuwait University and the University of York. The support of the research administration of Kuwait University to the XPS instrument (Project No. GS02/08) is acknowledged.

References

1- Y. Wang, I. Ramos, J. J. Santiago-Aviles, *J. Appl. Phys.*, 2007, **102**, 093517.

2- A. Eberheim, D. Kohl and P. Schieberle, *Phys. Chem. Chem. Phys.*, 2003, **5**, 5203–5206.

3- G. Gaggiotti, A. Galdikas, S. Kaciulis, G. Mattogno, A. Setkus, *J. Appl. Phys*., 1994, Vol. 76, **8**, 15.

4- V. A. Moshnikov, I. E. Gracheva, and M. G. An'chkov, *Glass Phys. Chem.*, 2011, **37**, 485.

5- C. J. Martinez, B. Hockey, C. B. Montgomery, S. Semancik, *Langmuir* 2005, **21***,* 7937.

6- Y. Zhang, Y. Liu, and M. Liu, C*hem. Mater.,* 2006, **18***,* 4643*.*

7- A.H. Whitehead, J.M. Elliott, J.R. Owen, *J. Power Sources*, 1999, **81–82**, 33.

8- Md. T. Uddin, Y. Nicolas, C. Olivier, T. Toupance, L. Servant, M. M. Müller, H.-J. Kleebe, J. Ziegler, and W. Jaegermann, *Inorg. Chem.*, 2012, **51**, 7764.

9- P. Zhu, M. V. Reddy, Y. Wu, S. Peng, S. Yang, A. S. Nair, K. P. Loh, B. V. R. Chowdari, S. Ramakrishna, *J. Mater. Chem.*, 2008, **18**, 771.

10- J. H. Pan, S. Y. Chai, C. Lee, S.-E. Park, W. I. Lee, *J. Phys. Chem. C,* 2007*,* **111**, 5582.

11- V. N. Urade and H. W. Hillhouse, *J. Phys. Chem. B,* 2005, **109**, 10538.

12- Y. Aksu, S. Frasca, U. Wollenberger, M. Driess, and A. Thomas, *Chem. Mater.*, 2011, **23**, 1798.

13- F. A. Garcés , L. N. Acquaroli, R. Urteaga, A. Dussan, R. R. Koropecki and R.D. Arce, *Thin Solid Films*, 2012, **520**, 4254.

14- H. Kim, J. Cho, *J. Mater. Chem.*, 2008, **18**, 771.

15- J. K. Shon, S. S. Kong, Y. S. Kim, J.-H. Lee, W. K. Park, S. C. Park, J. M. Kim, *Micropor. Mesopor. Mat.*, 2009, **120**, 441.

16- D. Chandra, N. Mukherjee, A. Mondal, and A. Bhaumik, *J. Phys. Chem. C*, 2008, **11***2,* 8668.

17- K. G. Severin, T. M. Abdel-Fattah and T. J. Pinnavaia, *Chem. Commun*., 1998, 1471.

18- X. Wang, S. S. Yee, W. P. Carey, *Sensors and Actuators*, B 24-25-1995,454-457

19- A. Dieguez, A. Romano-Rodringuez, J.R. Morante, U. Weimar, *Sens. Actuators B*, 1996, **31**, 1.

20- D. P. Tunstall, S. Patou, R. S. Liu, and Y. H. Kao, Mat. Res. Bull., 1999, **34**, 1513.

21- K. S. W. Sing, D. H. Everett, R. A. W. Haul, L. Mouscou, R. A. Pierottin, J. Rouquerol and T. Siemieniewska, 1985, *Pure Appl. Chem.*, 1985, **57**, 603.

22- Wenbo. B. Yue, Wuzong Z. Zhou, *Prog. Natural Sci.,* **18**, 1329, 2008.

23- Xianfeng Yang, Junxiang Fu, Chongiun Jin, Jian Chen, Chaolun Liang, Mingmei Wu, Wuzong Zhou, *J. Am. Chem. Soc.*, 2010, 132, **40**, pp 14279–14287.

24- The XPS data were interpreted based on the following website and the references contained therein: http://lasurface.com/database/elementxps.php.

25- Soumen Das, Dae-Young Kim, Cheol-Min Choi, Yoon-Bong Hahn, *Materials Research Bulletin*, **46** (2011) 609–614.